

# Influence of NaI background and mass on testing the DAMA modulation

Madeleine J. Zurowski<sup>1,2a</sup> and Elisabetta Barberio<sup>1,2</sup>

<sup>1</sup> School of Physics, University of Melbourne, Victoria, Australia

<sup>2</sup> ARC Centre of Excellence for Dark Matter Particle Physics

Received: date / Revised version: date

**Abstract.** We present here the model dependent and independent sensitivity studies for NaI detectors designed to test the DAMA result, and compare the predicted limits from SABRE with the present performance of both ANAIS and COSINE. We find that the strongest discovery and exclusion limits are set by a detector with the lowest background (assuming equal run times), and also note that our method correctly computes the present exclusion limits previously published by ANAIS and COSINE. In particular, with a target mass of 50 kg and background rate of 0.36 cpd/kg/keV (after veto), SABRE will be able to exclude the DAMA signal with  $3\sigma$  confidence or ‘discover’ it with  $5\sigma$  confidence within 2 years. This strongly motivates the quest for ever lower backgrounds in NaI detectors.

**PACS.** PACS-key describing text of that key

## 1 Introduction

There is a plethora of evidence that suggests some long-lived, non-luminous, particulate matter within the Universe. These cosmological observations exist on a wide range of scales, and there is no member of the Standard Model of Particle Physics (SM) able to successfully explain them all. As such, a new component called Dark Matter (DM) is required. Of the possible additions to the SM, the Weakly Interacting Massive Particle (WIMP) is one that has enjoyed popularity since its conception. This is due to the fact that particles on the weak scale have a self annihilation rate that naturally gives rise to the observed present day abundance of DM. Despite the fact that the standard assumptions for a WIMP (mass  $\sim$  GeV/ $c^2$ -TeV/ $c^2$ , cross section  $\sim 10^{-40}$  cm<sup>2</sup>) are now very heavily constrained experimentally, there are still a large number of experiments conducting searches for them.

WIMPs are typically probed for in one of three ways; indirect detection (observation of DM annihilation into SM particles), collider searches (observation of DM produced via SM annihilation), or direct detection (scattering of DM off some SM target). In particular, DM direct detection has a distinctive ‘smoking gun’ - a modulating interaction rate due to the relative velocity of the Earth and DM halo as the former rotates about the Sun. This modulation should be observed regardless of the particle interaction model considered as it depends only on the DM velocity distribution. Such a modulation should have a period of a year, and an amplitude of around 2% the constant rate.

One experiment has consistently observed such a signal over 14 annual cycles. Using a NaI target, the DAMA Collaboration has reported evidence of a DM consistent modulation with a combined statistical significance of  $12.9\sigma$  after around 15 years of data taking [1]. Despite this seemingly strong evidence, these results are in increasing tension with other direct detection experiments, which continue to publish null results for DM models that fit the DAMA data [2]. This has strongly constrained the standard WIMP assumptions, and pushed to more and more particular tailored models to explain these null results consistently.

The experiments that constrain the DAMA result depend largely on detectors that use a different scattering target, and as such, require the a priori assumption of some particular interaction model for analysis. In order to conclusively dismiss the DAMA signal as having a DM origin, it must be assessed in a model independent manner; that is, through the use of another NaI target experiment attempting to observe this annual modulation. At present, three such detectors are planned or already in the data taking stage: ANAIS, COSINE, and SABRE [3,4,5]. As these all use the same target as DAMA, under the assumption that all three experiments have a threshold efficiency and detector resolution similar to that of DAMA, they are expected to be able to observe the same modulation signal, given a low enough background and long enough data taking period. Thus, model independent sensitivity limits can be constructed in the background-lifetime plane similar to how they are in the  $m_\chi$ - $\sigma_0$  plane in the model dependent case. This allows for a comparison of the performance of the three NaI detectors given their different

<sup>a</sup> madeleine.zurowski@unimelb.edu.au

background and exposure masses.

This paper commences by detailing the method used to carry out both model dependent and independent sensitivity calculations in Section 2. It then presents the results of both sensitivity cases, and compares the exclusion and discovery powers of ANAIS, COSINE, and SABRE in Section 3, before concluding in Section 4.

## 2 Sensitivity methodology

In general, an experiment will be sensitive to a DM modulating signal if the signature modulation is observable over the detectors background. In this case, the apparent modulation of the background signal due to statistical fluctuations is more problematic than the background rate itself, as analysis of the modulation signature typically involves the subtraction of the constant signal component. As such, to assess the sensitivity of a detector, these fluctuations should be modelled over its lifetime, and fit to a cosine function to find the probability of this masking or mimicking the DM signal.

Assuming that in some energy bin of width  $\Delta E$  over a time period of  $\Delta T$ , the observed background rate is given by  $R_b$  (in units of cpd/kg/keV), these background statistical fluctuations can be modelled by sampling from a Poisson distribution centred on

$$N_b = M_E \times \Delta T \times \Delta E \times R_b, \quad (1)$$

where  $M_E$  is the mass of the detector in question. The signal plus background (s + b) modulation can be modelled in a similar way, sampling instead from

$$N_{s+b} = M_E \times \Delta T \times \Delta E \times (R_b + R_0 + R_m \cos \omega t), \quad (2)$$

where  $R_0$  and  $R_m$  are the constant and modulating signal events observed in a given energy bin. Generating this for every live bin period of detector operation, the total observed rate is then fit to  $R(t) = R_c + R_f \cos \omega t$  in order to separate the constant ( $R_c$ ) and fluctuating ( $R_f$ ) components. A non-zero modulation can be seen in both the background only and signal plus background cases - see, for example, Figs. 1 and 2, where a 50 kg detector running for 3 years observes a signal compatible with  $R_f = 23.3 \pm 18.8$  counts per month for background only, and  $R_f = 83.8 \pm 24.5$  counts per month for signal plus background. Note also that in both cases, the observed signal is incompatible with zero modulation.

This modulation is then generated a number of times ( $\mathcal{O}(100-1000)$ ), saved, and fit to a gaussian corresponding to the probability of observing a given modulation amplitude for either the background only or signal+background case. These distributions are then compared to assess the ability of the detector to distinguish between the two models. Samples of these can be seen in Fig. 3, where  $R_0$  and  $R_m$  are DAMA observations from Ref. [1]. Thus, the tuneable parameters to assess the sensitivity of a detector are the run time, detector background,  $R_m$ , and  $R_0$ . Typical model dependent analyses will set  $R_b$  and the run time

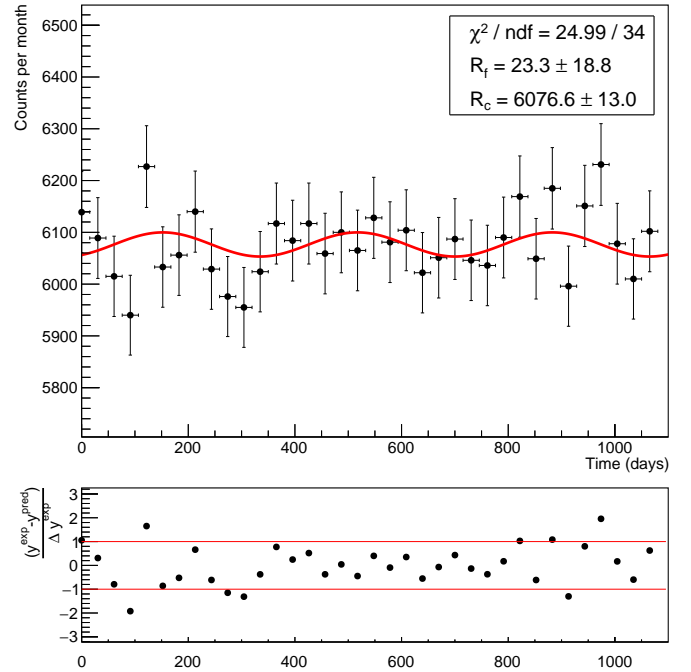


**Fig. 1.** Simulated fluctuations in background only model, with  $R_b = 1$  cpd/kg/keV over 3 years fit to  $R(t) = R_c + R_f \cos \omega t$ .

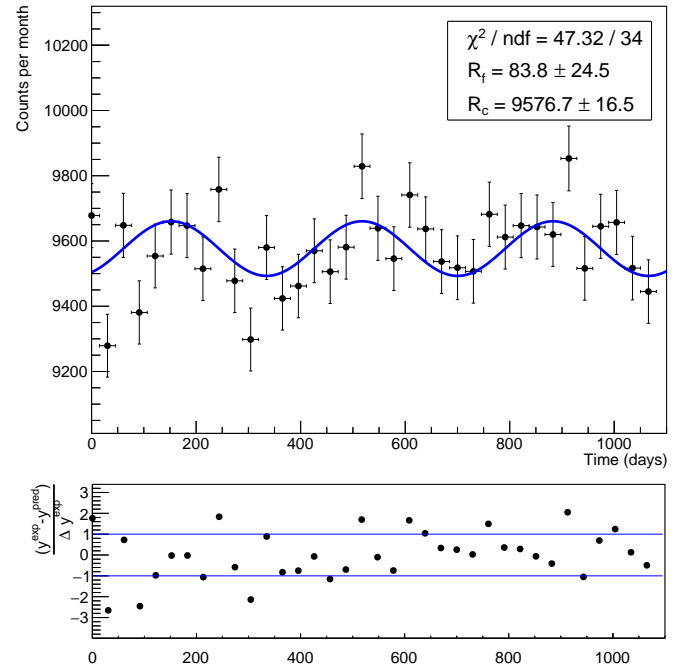


**Fig. 2.** Simulated fluctuations in signal+background model, with  $R_b = 1$  cpd/kg/keV and DAMA signal rate over 3 years fit to  $R(t) = R_c + R_f \cos \omega t$ .

based on the detector in question, and vary  $R_m$  and  $R_0$  by setting different values of  $m_\chi$  and  $\sigma_0$ . However, it is also possible to set  $R_m$  and  $R_0$ , (to the values observed by DAMA, for example) and vary the detector parameters to find the required lifetime and background for a

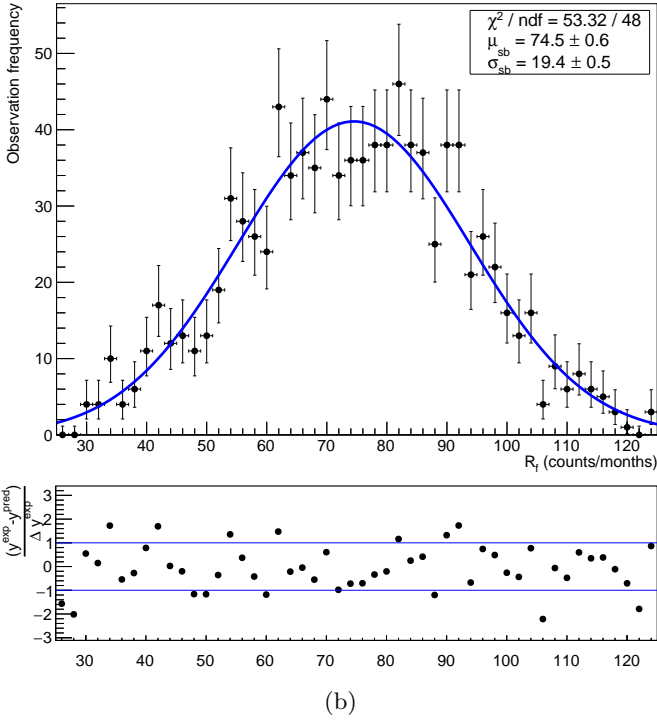
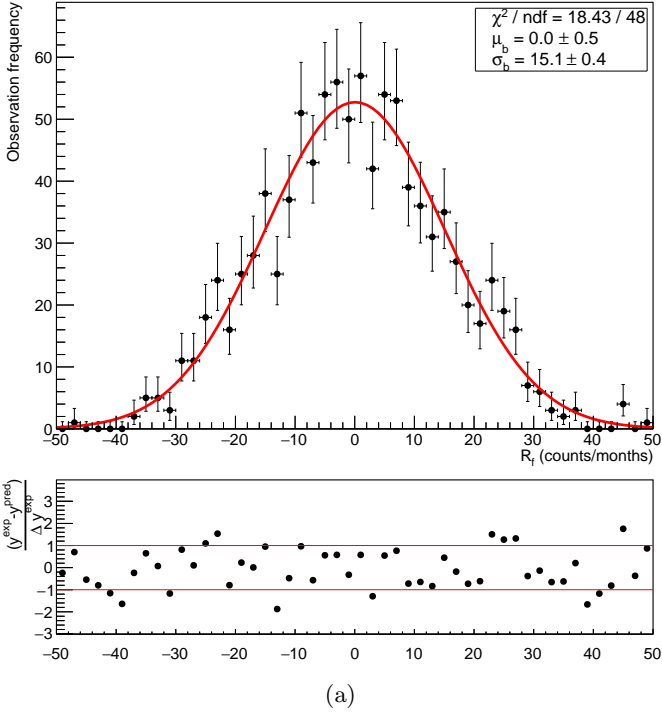


**Fig. 3.** Background only (top) and signal+background (bottom) distributions, for  $R_b = 1$  cpd/kg/keV over 3 years, and signal given by DAMA. These are plotted as a function of the number of modulation events observed per month.

detector to observe this particular signal, rather than a specific DM model. The test statistic we will use to assess detector sensitivity is the  $\sigma$  confidence level, where here  $\sigma$  is the standard deviation of the signal+background gaus-

sian [6]. In the event of a null results, the detector will exclude some model/combination of  $R_m$  and  $R_0$  with  $n\sigma$  confidence, where

$$n = \frac{|\mu_{sb} - \mu_b|}{\sigma_b}. \quad (3)$$

Here,  $\mu_b$  ( $\mu_{sb}$ ) corresponds to the mean modulation observed by the background (signal+background) model. Where we want to plot the 90% CL in the  $m_\chi - \sigma_0$  plane, as is standard for model dependent sensitivity plots, we compute the one sided p-value associated with  $n$ ,

$$p = \frac{1}{2} \left( 1 - \operatorname{erf} \left( \frac{n}{\sqrt{2}} \right) \right), \quad (4)$$

and require that  $p \leq 0.1$ .

If instead we are interested in the discovery power rather than the exclusion (the probability that observation of  $\mu_{sb}$  can occur in data generated by the background only model), the  $\sigma$  confidence level will depend on the uncertainty of the background only distribution, and be given by

$$n = \frac{|\mu_{sb} - \mu_b|}{\sigma_b}. \quad (5)$$

## 2.1 Assumptions

For both the model dependent and independent sensitivity calculations, we make a number of assumptions for ease of computation and comparison across different detectors. They are compiled in this section for reference. In all cases, we consider three detectors, with the exposure mass and backgrounds reported by ANAIS and COSINE, and those planned for SABRE, given in Table 1 with those reported by DAMA for comparison.

**Table 1.** Detector properties.

Experiment	Mass (kg)	$R_b$ (dru)
ANAIS	112	3.2 [7]
COSINE	57.5	2.7 [8]
DAMA	250	0.8 [9]
SABRE	50	0.36 [10]

### 2.1.1 Model dependent assumptions

The expression we use for the DM interaction rate as a function of nuclear recoil is

$$\frac{dR}{dE_R} = N_T \frac{\rho}{m_\chi} \int v f_{\text{lab}}(\vec{v}) \frac{d\sigma_T}{dE_R} d^3v, \quad (6)$$

where the dependence on model choice comes from the selection of normalised couplings constants  $\hat{c}_i^{(a)} \hat{c}_j^{(b)}$  in

$$\frac{d\sigma_T}{dE_R} = \frac{m_T \sigma_0}{2v^2 \mu_N^2} \left[ \sum_{i,j} \sum_{a,b=0,1} \hat{c}_i^{(a)} \hat{c}_j^{(b)} F_{ij}^{(ab)}(v, q) \right]. \quad (7)$$

For the simple spin independent model we use here, we take all couplings as non-zero, save for  $c_1^{(0)} = 1$ , while the form factors used are taken from the appendix of Ref.[11]. Under these assumptions, the differential cross section simplifies to

$$\begin{aligned} \frac{d\sigma_T}{dE_R} &= \frac{m_T}{2v^2} \frac{\sigma_0}{\mu_N^2} F_{11}^{(00)}(q) \\ &= \frac{m_T}{8v^2} \frac{\sigma_0}{\mu_N^2} \left( F_{11}^{(p,p)}(q) + F_{11}^{(n,n)}(q) + 2F_{11}^{(n,p)}(q) \right). \end{aligned} \quad (8)$$

The expressions for these nuclear form factors for  $^{23}\text{Na}$  and  $^{127}\text{I}$  are given in Appendix A.

We also assume the standard halo model for the velocity distribution,

$$f_{lab}(v) = \frac{1}{(\pi v_0^2)^{3/2}} \exp \left[ -\frac{1}{v_0^2} (\mathbf{v} - \mathbf{v}_E)^2 \right], \quad (9)$$

where  $v_0 = 220 \text{ km s}^{-1}$ ,  $v_{\text{esc}} = 550 \text{ km s}^{-1}$ , and  $\rho = 0.3 \text{ GeV cm}^{-3}$ . The Earth's velocity  $\mathbf{v}_E$  is given by  $\mathbf{v}_E = \mathbf{v}_\odot + \mathbf{v}_t$ , where

$$\begin{aligned} \vec{v}_\odot &= v_\odot(0, 0, 1), \\ \vec{v}_t &= v_t(\sin 2\pi t, \sin \gamma \cos 2\pi t, \cos \gamma \cos 2\pi t), \\ v_\odot &= 232 \text{ kms}^{-1}, \\ v_t &= 30 \text{ kms}^{-1}, \\ \gamma &= \pi/3 \text{ rad}. \end{aligned} \quad (10)$$

For the detector specific response functions, we assume that all three detectors of interest have the same quenching factors as DAMA ( $Q_{Na} = 0.3$  and  $Q_I = 0.09$ ), as well as the energy resolution given in Ref.[12]:

$$\sigma_E = \left( 0.0091 \frac{E_{ee}}{\text{keVee}} + 0.488 \sqrt{\frac{E_{ee}}{\text{keVee}}} \right) \text{ keV}, \quad (11)$$

and the detector resolution as in Ref. [13]:

$$\epsilon(E) = \begin{cases} 0.0429E + 0.657 & \text{for } E < 8 \text{ keV} \\ 1 & \text{otherwise} \end{cases}. \quad (12)$$

Thus, the observed rate in a given energy bin of width  $\Delta E = 2\delta E$  is

$$\begin{aligned} \Delta E \times R(E) &= \int_{E-\delta E}^{E+\delta E} \frac{dR}{dE'} dE', \quad \text{where} \\ \frac{dR}{dE'} &= \frac{\epsilon(E')}{Q_T} \frac{1}{(2\pi)^{1/2}} \int_0^\infty \frac{dE_{ee}}{\sigma_{E_{ee}}} \frac{dR}{dE_R} \exp \left[ \frac{-(E' - E_{ee})^2}{2(\sigma_{E_{ee}})^2} \right]. \end{aligned} \quad (13)$$

This can be split into the constant and modulating components by projecting onto a cosine function with the expected period and offset for DM.

### 2.1.2 Model independent assumptions

For the model independent analysis, we assume that all detectors should observe exactly the same rate as reported by DAMA. In that case we can take the signal rate to be  $R(t) = S_0 + S_m \cos \omega t$  for the reported bins, where  $S_m$  is given explicitly in Ref. [1], and  $S_0$  is inferred from the fact that for the SHM velocity distribution (which dictates modulation of signal)  $S_m/S_0 \simeq 0.02$ . This method of extracting  $S_0$  is only an approximation. More correct results could be generated using the exact constant rate observed, if available. The relevant rates are given here in Table 2.

**Table 2.** Modulating and inferred constant DAMA rates [1].

Energy (keV)	$S_m$ (cpd/kg/keV)	$S_0$ (cpd/kg/keV)
1.0 - 1.5	$0.0232 \pm 0.0052$	1.160
1.5 - 2.0	$0.0164 \pm 0.0043$	0.820
2.0 - 2.5	$0.0178 \pm 0.0028$	0.890
2.5 - 3.0	$0.0190 \pm 0.0029$	0.950
3.0 - 3.5	$0.0178 \pm 0.0028$	0.890
3.5 - 4.0	$0.0109 \pm 0.0025$	0.545
4.0 - 4.5	$0.0110 \pm 0.0022$	0.550
4.5 - 5.0	$0.0040 \pm 0.0020$	0.200
5.0 - 5.5	$0.0065 \pm 0.0020$	0.325
5.5 - 6.0	$0.0066 \pm 0.0019$	0.330

## 3 Results

Our sensitivity results are split into two sections, model dependent and independent. The former are the more traditional presentation, selecting a model (here, the 'standard' spin independent elastic WIMP) and varying  $m_\chi$  and  $\sigma_0$  - equivalent to changing  $R_m$  and  $R_0$ . The latter demonstrate the exclusion power of various NaI experiments as a function of their runtime, setting  $R_m$  and  $R_0$  to the values reported by DAMA.

### 3.1 Model dependent

The choice of a particular model will dictate the observable  $R_m$  and  $R_0$  for some combination of DM mass and cross section,  $m_\chi$  and  $\sigma_0$ . To produce the usual sensitivity curves, we loop through a set range of  $m_\chi$  and  $\sigma_0$ , and compute the p-values of  $\mu_b$  (the mean of the background only distribution) in the signal+background distribution. A detector will be sensitive with 90% confidence to the combinations that produce  $P(x = \mu_b) \leq 0.1$ .

The results of applying this method for ANAIS, COSINE, and SABRE after 3 years of operation are shown in Fig. 4 for the standard spin independent DM model, compared with DAMA run for the same period of time. This demonstrates that although all the detectors have

the same target, there are still combinations of DM parameter space that will produce a statistically significant modulation in some detectors, but not in others over the same run time.

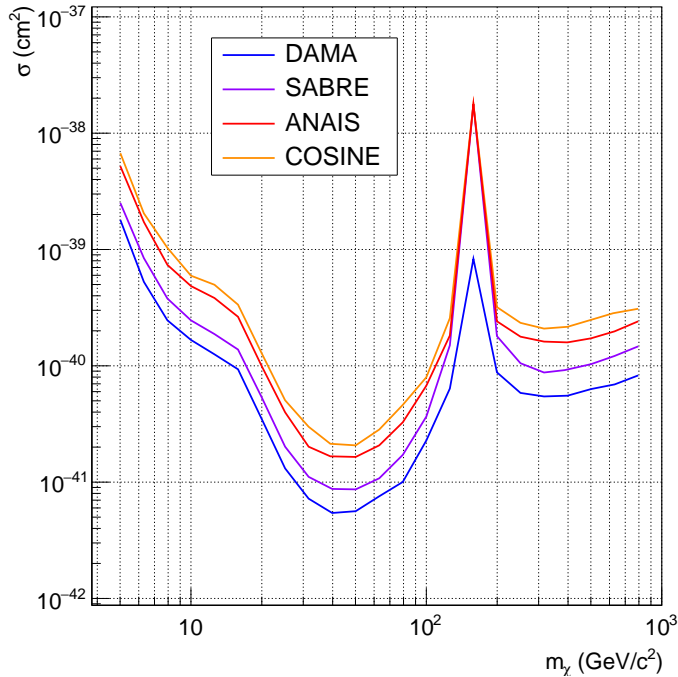


**Fig. 4.** 90 % C.L. modulation sensitivity of various NaI detectors after 3 years of operation, assuming a spin independent elastic WIMP. For each detector the exposure mass and  $R_b$  are shown in Table 1.

Note that the peak occurring at  $m_\chi \sim 150 \text{ GeV}/c^2$  is due to our assumption of a single energy bin from 2-6  $\text{keV}^1$ . At this mass range the net modulation in our energy region of interest switches from positive to negative, and so averaging over the energy bins erroneously gives a modulation amplitude close to zero, drastically reducing the sensitivity. See, for example, Fig. 5. More proper analysis requires knowledge of the background energy spectrum not publicly available.

The exposure mass and detector backgrounds assumed for this analysis are given in Table 1. Interestingly, despite having the lowest target mass, SABRE has the greatest sensitivity of the three new detectors to the annual modulation of these models across the full parameter space. This is likely due its low background, which is projected to be approximately an order of magnitude lower than that of ANAIS, the next most sensitive detector. Where backgrounds are of a similar scale, as for COSINE and ANAIS with 2.7 and 3.2  $\text{cpd}/\text{kg}/\text{keV}$  respectively, the exposure mass becomes more important - here the fact that

<sup>1</sup> We make this assumption to remain agnostic about the exact background energy spectrum of the three detectors, as all have published only a single value for the 2-6 keV range.

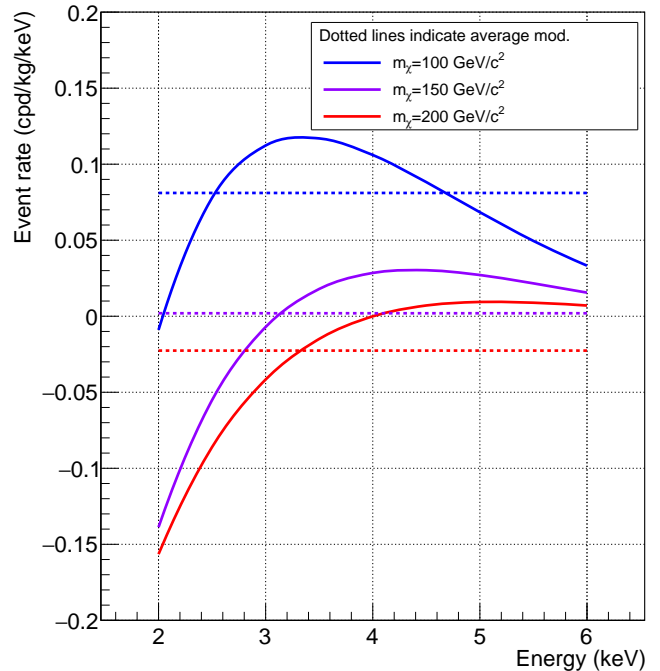


**Fig. 5.** Modulation rate both as a spectrum and averaged over the region of interest for various DM masses and  $\sigma_0 = 10^{-39} \text{ cm}^2$ .

ANAIS uses almost double the mass of COSINE for analysis gives it a slight edge. Similarly, DAMA's exposure mass (5 times the size of SABRE's) gives it the largest sensitivity region.

Although increasing a detectors target mass increases the number of DM events, it will also increase the number of background events by the same scale. Thus although there is some improvement in sensitivity in this case, reducing the background appears to be a far more effective way of improving detector performance - at least for the standard WIMP model assumed here. This is what allows SABRE to approach the limit set by DAMA much closer than either ANAIS or COSINE.

The analysis described in this section is typical in the production of exclusion plots, and is the only way to compare detectors using different targets. The downside of this method is that it remains possible to tailor increasingly complex DM models to explain the lack of a modulating signal at detectors other than DAMA. To properly exclude (or support) this observation, we need to understand and compare the exclusion power of other NaI detectors for the DAMA rate, in the event they return null results.

### 3.2 Model independent

Detectors that use the same target should theoretically all observe the same interaction rate. In reality, the efficiency and resolution may cause some variation between detectors, but we can consider the DAMA data a minimum observable rate, as the newer detectors tend to improve

upon both values [14,15], particularly above 2 keV. We can take advantage of this, and instead of assuming some model, DM mass, and cross section to construct  $R_m$  and  $R_0$ , we use the DAMA values given in Ref.[1], which should also be visible at other NaI detectors. Using this, we can find the  $n\sigma$  confidence level exclusion or discovery power of the DAMA rate after a given run time.

The exclusion power of the various NaI detectors is shown in Fig. 6, discovery power in Fig. 7, and the properties assumed for each of detector are given in Table 1. Key and present sensitivity milestones are also shown in Table 3. These results again assume a single energy bin from 2-6 keV, and a constant background over that region as reported in the provided references. We also note that the present and predicted exclusion power we find for both ANAIS and COSINE are consistent with those previously presented by both collaborations [3,8].

**Table 3.** Present exclusion C.L. for the detectors, and years for significant exclusion (Fig. 6) and discovery C.L. (Fig. 7).

Exp.	Present excl.	For $3\sigma$ excl.	For $5\sigma$ disc.
ANAIS	$2.5\sigma$	$\sim 3$ yrs	$\sim 7$ yrs
COSINE	$1.6\sigma$	$\sim 5$ yrs	$> 7$ yrs
SABRE	0	$\sim 2$ yrs	$\sim 2$ yrs

For this model independent analysis, we see the same trend as in Fig. 4, where the low background of SABRE makes it the most sensitive experiment, despite also having the lowest target mass. This is even more obvious considering the exclusion vs. discovery plots. As explained in Sec 2 in Eq. 3 and 5, the former depends on the uncertainty in *signal+background*, while the latter relies only on *background* uncertainty. As such, the improvements from lowering the background are much clearer in the case of discovery power, which explains why the SABRE experiment is able to perform so much better than COSINE and ANAIS.

Focusing on the discovery plot in Fig. 7, this gives the significance of a modulating signal compatible with DAMA's, should it be observed by any of the detectors. Comparing the three experiments at any given time, we find that

$$\sigma \text{ C.L.} \propto \sqrt{\frac{M_E}{R_b}}. \quad (14)$$

Thus, with their present reported backgrounds, ANAIS and COSINE would require exposure masses of 445 kg and 375 kg respectively to reach the  $5\sigma$  discovery at the same time as SABRE. Clearly, a lower background gives a significant advantage, in terms of time the experiment needs for statistically significant results, as well as the laboratory space it will ultimately take up.

### 3.3 Mass and background requirements

The model independent sensitivity method can also be used to compute the mass and background required for a

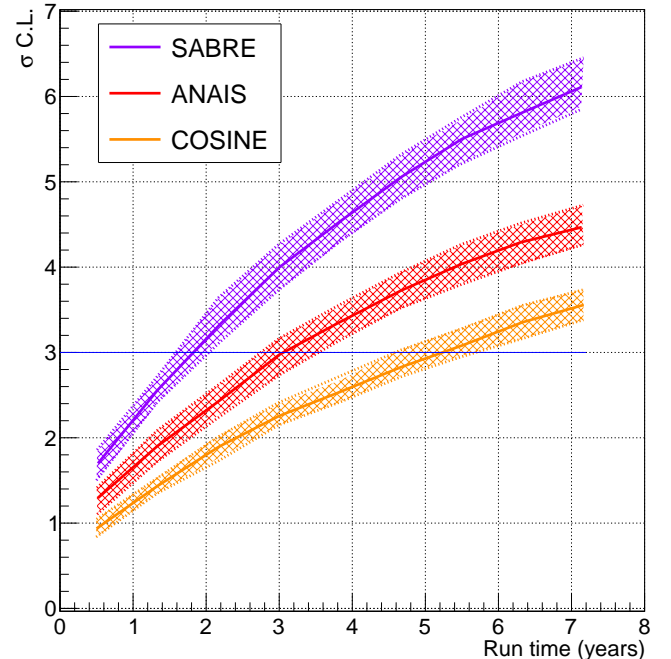


**Fig. 6.** Exclusion power of NaI detectors, as a function of run time. Cross hatched regions indicated  $1\sigma$  uncertainty bands. Blue line indicates typical benchmark value.

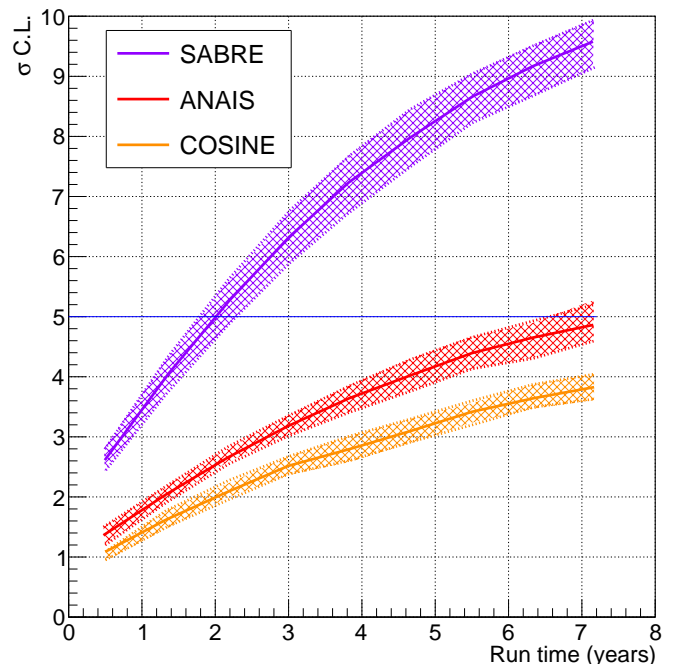


**Fig. 7.** Discovery power of NaI detectors, as a function of run time. Cross hatched regions indicated  $1\sigma$  uncertainty bands. Blue line indicates typical benchmark value.

detector to exclude the DAMA results with a given confidence level within a specified period of time. For example, assuming that we want an experiment to have exclusion power of  $3\sigma$  within three years, we can plot the maximum

allowable background that will give this sensitivity as a function of exposure mass. Alternatively, it can be used to find the minimum exposure mass in the event we cannot get below some particular background threshold.

These results are given in Fig. 8. If a collaboration has only enough time/resources to grow  $\sim 65$  kg of crystal, they will require an experiment background of below 1.5 cpd/kg/keV in order to have  $3\sigma$  exclusion power of the the DAMA signal within three years. Conversely, if they know they are able to achieve a background of 0.5 cpd/kg/keV, they need only about 30 kg of crystal for the same time and sensitivity requirements.

Calculations and plots of this kind may prove useful at the R&D or upgrade stages of NaI detectors to inform or validate choices made surrounding target masses and background reduction.

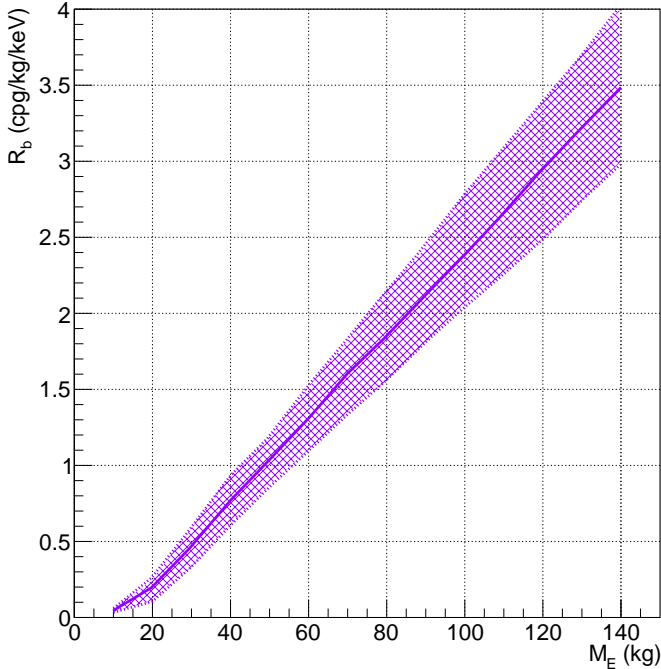


**Fig. 8.** Maximum background and minimum mass combinations that provide  $3\sigma$  exclusion of DAMA within three years of operation. Hatched bands give  $1\sigma$  uncertainty. If a detector's properties fall below the line, it will have the requisite sensitivity.

## 4 Conclusions

We have presented here the comparative sensitivity of NaI detectors computed in both a model dependent and independent way. In both cases, for both exclusion and discovery limits the lowest background experiment (SABRE) has performed the best of the three experiments, despite being the one with the lowest exposure mass. This makes clear just how important a low background is for DM searches such as these, in order to observe the small modulation in an already low interaction rate. This further motivates the purification and veto techniques presently explored by these collaboration. Should the projected exposure mass and backgrounds be achieved, and data taking commence in the next 18 months, SABRE will be positioned to provide statistically significant exclusion or discovery of the DAMA signal within 3-4 years, either in tandem or ahead of COSINE or ANAIS.

In this event (and even more so in the event of a positive DM-like signal), it will be perhaps beneficial and interesting to compare the results of the Northern and Southern hemisphere experiments and data, to further elucidate clues as to nature of the modulating DAMA signal - DM or not.

## Acknowledgments

The authors would like to thank Phillip Urquijo for his review of the paper. This work was supported by the ARC Centre of Excellence of Dark Matter Particle Physics through grant CE200100008. MJZ is also supported through the Australian Government Research Training Program Scholarship. Both authors are members of the SABRE collaboration.

## A Nuclear form factors

These form factors are given in terms of the dimensionless  $y = (qb/2)^2$ , where  $b$  is the harmonic oscillator parameter:

$$b = \sqrt{\frac{41.467}{45A^{-1/3} - 25A^{-2/3}}} \text{ fm.} \quad (15)$$

$^{23}\text{Na}$ :

$$\begin{aligned} F_{11}^{(p,p)}(q) &= e^{-2y} (120 - 180y + 87y^2 - 17y^3 + 1.2y^4) \\ F_{11}^{(p,n)}(q) &= e^{-2y} (130 - 200y + 100y^2 - 20y^3 + 1.5y^4) \\ F_{11}^{(n,n)}(q) &= e^{-2y} (140 - 220y + 120y^2 - 25y^3 + 1.8y^4) \end{aligned} \quad (16)$$

$^{127}\text{I}$ :

$$\begin{aligned} F_{11}^{(p,p)}(q) &= e^{-2y} (2800 - 10000y + 14000y^2 - 9800y^3 \\ &\quad + 3800y^4 - 840y^5 + 100y^6 - 6.3y^7 + 0.15y^8) \\ F_{11}^{(p,n)}(q) &= e^{-2y} (3900 - 15000y + 23000y^2 - 18000y^3 \\ &\quad + 7900y^4 - 2000y^5 + 290y^6 - 23y^7 + 0.75y^8 \\ &\quad - 0.0048y^9) \\ F_{11}^{(n,n)}(q) &= e^{-2y} (5500 - 23000y + 38000y^2 - 32000y^3 \\ &\quad + 16000y^4 - 4600y^5 + 790y^6 - 75y^7 + 3.3y^8 \\ &\quad - 0.041y^9 + 0.00015y^{10}) \end{aligned} \quad (17)$$

## References

1. R. Bernabei et al., [The DAMA Collaboration], *First Model Independent Results from DAMA/LIBRA-Phase2*, *Universe* **4** (2018) no. 11, 116, [arXiv:1805.10486 \[hep-ex\]](#). [Nucl. Phys. Atom. Energy19,no.4,307(2018)].
2. M. Tanabashi et al., Particle Data Group, *Review of Particle Physics*, *Phys. Rev. D* **98** (2018) no. 3, 030001.
3. [The ANAIS Collaboration], J. Amare et al., *Annual Modulation Results from Three Years Exposure of ANAIS-112*, Preprint, 2021. [arXiv:2103.01175 \[astro-ph.IM\]](#).
4. [The COSINE Collaboration], G. Adhikari et al., *Strong constraints from COSINE-100 on the DAMA dark matter results using the same sodium iodide target*, Preprint, 2021. [arXiv:2104.03537 \[hep-ex\]](#).
5. M. Antonello et al., [The SABRE Collaboration], *The SABRE project and the SABRE Proof-of-Principle*, *Eur. Phys. J.* **C79** (2019) no. 4, 363, [arXiv:1806.09340 \[physics.ins-det\]](#).
6. G. Cowan, K. Cranmer, E. Gross, and O. Vitells, *Asymptotic formulae for likelihood-based tests of new physics*, *The European Physical Journal C* **71** (2011) no. 2, . <http://dx.doi.org/10.1140/epjc/s10052-011-1554-0>.
7. J. Amare et al., [The ANAIS Collaboration], *Analysis of backgrounds for the ANAIS-112 dark matter experiment*, *Eur. Phys. J.* **C79** (2019) no. 5, 412, [arXiv:1812.01377 \[astro-ph.GA\]](#).
8. G. Adhikari and et al., [The COSINE Collaboration], *Search for a Dark Matter-Induced Annual Modulation Signal in NaI(Tl) with the COSINE-100 Experiment*, *Physical Review Letters* **123** (2019) no. 3, . <http://dx.doi.org/10.1103/PhysRevLett.123.031302>.
9. R. Bernabei et al., *The DAMA project: Achievements, implications and perspectives*, *Progress in Particle and Nuclear Physics* **114** (2020) 103810. <https://www.sciencedirect.com/science/article/pii/S0146641020300570>.
10. M. Antonello et al., [The SABRE Collaboration], *Monte Carlo simulation of the SABRE PoP background*, *Astropart. Phys.* **106** (2019) 1–9, [arXiv:1806.09344 \[physics.ins-det\]](#).
11. N. Anand, A. L. Fitzpatrick, and W. C. Haxton, *Weakly interacting massive particle-nucleus elastic scattering response*, *Phys. Rev.* **C89** (2014) no. 6, 065501, [arXiv:1308.6288 \[hep-ph\]](#).
12. R. Bernabei et al., [The DAMA Collaboration], *The DAMA/LIBRA apparatus*, *Nucl. Instruments Methods Phys. Res. Sect. A Accel. Spectrometers, Detect. Assoc. Equip.* **592** (2008) no. 3, 297–315.
13. R. Bernabei et al., [The DAMA Collaboration], *The DAMA/LIBRA apparatus*, *Nucl. Instrum. Meth.* **A592** (2008) 297–315, [arXiv:0804.2738 \[astro-ph\]](#).
14. [The COSINE Collaboration], G. Adhikari and et al., *Lowering the energy threshold in COSINE-100 dark matter searches*, Preprint, 2020. [arXiv:2005.13784 \[physics.ins-det\]](#).
15. J. Amaré et al., [The ANAIS Collaboration], *Performance of ANAIS-112 experiment after the first year of data taking*, *The European Physical Journal C* **79** (2019) no. 3, . <http://dx.doi.org/10.1140/epjc/s10052-019-6697-4>.